

# Upper critical field in electron-doped cuprate superconductor $\text{Nd}_{2-x}\text{Ce}_x\text{CuO}_{4+\delta}$ : two-gap model

T.B.Charikova<sup>a1</sup>, N.G.Shelushinina<sup>a</sup>, G.I.Harus<sup>a</sup>, D.S.Petukhov<sup>a</sup>,  
V.N.Neverov<sup>a</sup>, A.A.Ivanov<sup>b</sup>

<sup>a</sup>*Institute of Metal Physics RAS, Ekaterinburg, Russia,*

<sup>b</sup>*Moscow Engineering Physics Institute, Moscow, Russia*

---

## Abstract

We present resistivity measurements of the upper critical field ( $H_{c2}$ ) phase diagram as a function of temperature (T) for  $\text{Nd}_{1.85}\text{Ce}_{0.15}\text{CuO}_{4+\delta}/\text{SrTiO}_3$  single crystal films with different degree of disorder ( $\delta$ ) in magnetic fields up to 90 kOe at temperatures down to 0.4 K. The data are well described by a two-band/two-gap model for a superconductor in the dirty limit.

*Keywords:* Cuprate superconductors, Upper critical field, Two-gap model

---

## 1. INTRODUCTION

The theory of the two-band superconductivity has been developed more than 50 years ago: Suhl, Matthias, and Walker [1] predicted the existence of *multigap* superconductivity, in which a distinction of the pairing interaction in different bands leads to different order parameters and to an enhancement of the critical temperature.

A discovery of  $\text{MgB}_2$  has renewed interest in superconductors with multicomponent order parameters.  $\text{MgB}_2$  seems to be the first superconductor for which a two-gap model offers a simple explanation of many anomalous experimental findings. The two-band model for superconductivity in  $\text{MgB}_2$  was first suggested in [2,3]. On the basis of first-principles calculations of the electronic structure and the electron-phonon interaction, it was argued that superconductivity in this compound resides in two groups of bands: the

---

<sup>1</sup>charikova@imp.uran.ru

group of two strongly superconducting  $\sigma$ -bands and the group of two weakly superconducting  $\pi$ -bands.

A theory for the upper critical field  $H_{c2}$  of two-gap superconductors in the dirty limit is developed by Gurevich [4] on the ground of a multiband BCS model [1]. The equations for  $H_{c2}$  for two-band superconductors in the dirty limit are derived with the account of both intraband and interband scattering by nonmagnetic impurities. It is shown that the shape of the  $H_{c2}(T)$  curve essentially depends on the ratio of the intraband electron diffusivities  $D_1$  and  $D_2$ , and can be very different from the one-gap dirty-limit theory. Taking  $\text{MgB}_2$  as an example, the results of this work are used to describe the observed abnormal temperature dependences of  $H_{c2}$  of this compound.

The discovery of oxypnictides as a new class of superconductors [5] has regenerated interest in high temperature superconductivity. It is shown by Mazin et al. [6] that the pairing mechanism in iron arsenide pnictides is consistent with the multi-band theory: the so-called “extended  $s_{\pm}$  -wave” model with a sign reversal of the order parameter between different sheets of Fermi surface. The relatively high upper critical fields ( $H_{c2}$ ) with atypical temperature dependence in these materials immediately attracted much interest. In particular, the anomalous upward curvature observed in the temperature dependence of  $H_{c2}$  in these materials made the dirty two-band model [4] used to describe  $\text{MgB}_2$  a natural and useful choice [7-11]. The model of Gurevich [4] is widely exploited for describing of a variety of the abnormal  $H_{c2}$  temperature dependences, both for  $H \parallel c$  and  $H \perp c$ , in  $\text{NdFeAsO}_{0.7}\text{F}_{0.3}$  single crystals [7], in polycrystalline  $\text{LaFeAsO}_{0.89}\text{F}_{0.11}$  samples [8], in cobalt-doped  $\text{SrFe}_2\text{As}_2$  epitaxial films [9], in Co-doped  $\text{BaFe}_2\text{As}_2$  single crystals [10] and in  $\text{Sr}_{1-x}\text{Eu}_x(\text{Fe}_{0.89}\text{Co}_{0.11})_2\text{As}_2$  single crystals ( $x = 0.20$  and  $0.46$ ) [11].

An anomalous upward curvature of  $H_{c2}(T)$  dependence has been reported in the earliest investigations of electron-doped superconducting  $\text{Nd}_{2-x}\text{Ce}_x\text{CuO}_{4+\delta}$  crystals [12, 13]. Such a non-BCS behavior of  $H_{c2}(T)$  was observed later both in  $\text{Nd}_{2-x}\text{Ce}_x\text{CuO}_{4+\delta}$  single crystals [14] and thin films [15, 16].

Gantmacher et al. [14] have argued that the observed concave form of  $H_{c2}(T)$  in their bulk  $\text{Nd}_{1.82}\text{Ce}_{0.18}\text{CuO}_{4+\delta}$  crystals may be an indication of unconventional boson-type superconductivity. In the work of Golnik and Naito [15] it is shown that the normal state resistivity, Hall coefficient and magnetoresistivity of  $\text{Nd}_{2-x}\text{Ce}_x\text{CuO}_{4+\delta}$  films can be described quantitatively within a simple two-carrier model if the existence of an electronlike and a holelike band is assumed. The physical origin of the two conduction bands at that time remained an open question. In the superconducting regime the

positive curvature of the resistive critical field was attributed by them to the quasi-2D character of the material and the resulting fluctuation effects.

There are much recent activities in investigation of possible electrons and holes coexistence in the normal state of cuprate superconductors [17]. Two kinds of carriers in electron-doped cuprates with different lanthanide cations seem to arise from the electronic structure near the Fermi surface (FS) of the  $\text{CuO}_2$  planes. Angle resolved photoemission spectroscopy (ARPES) has revealed a small electron-like FS pocket in the underdoped region, and a simultaneous presence of both electron- and hole-like pockets near optimal doping in  $\text{Nd}_{2-x}\text{Ce}_x\text{CuO}_{4+\delta}$  systems [18,19]. The conclusions of the ARPES measurements and first-principle calculations of the electronic structure on the electron-doped high-Tc superconductors  $\text{Ln}_{1.85}\text{Ce}_{0.15}\text{CuO}_4$  ( $\text{Ln} = \text{Nd}, \text{Sm}$  and  $\text{Eu}$ ) performed by Ikeda et al. [20], are in accordance with these results. A spin density wave (SDW) model [21-23] was proposed which gives qualitative explanation to ARPES observations. In this model, SDW ordering would induce FS reconstruction that results in an evolution from an electron pocket to the coexistence of electron-like and hole-like pockets and then into a single hole-like FS with increasing of doping.

In our previous work [24] we have analyzed the Ce -doping dependence of the normal state Hall coefficient in optimally reduced  $\text{Nd}_{2-x}\text{Ce}_x\text{CuO}_{4+\delta}/\text{SrTiO}_3$  single crystal films and, on the grounds of this analysis, we have recruited a two-carrier model for describing of the mixed state Hall coefficient. We have adopted a semi-phenomenological description of a mixed state Hall effect by flux-flow model of Bardeen and Stephen modified by coexistence of electrons and holes. In this work we present results on the upper critical field as a function of temperature determined by a resistive method in  $\text{Nd}_{2-x}\text{Ce}_x\text{CuO}_{4+\delta}/\text{SrTiO}_3$  single crystal films with  $x=0.15$  and various degree of disorder ( $\delta$ ). Our goal is to describe the observed abnormal  $H_{c2}$  (T) dependences on the ground of two-gap model of Gurevich [4]. Such an approach may occur actual in the light of much recent efforts on experimental (ARPES) and theoretical (SDW-model) investigations of the electronic structure near Fermi surface in the  $\text{CuO}_2$  plane of electron-doped cuprate superconductors.

## 2. SAMPLES AND EQUIPMENT

The series of  $\text{Nd}_{2-x}\text{Ce}_x\text{CuO}_{4+\delta}/\text{SrTiO}_3$  epitaxial films ( $x = 0.15$ ) with standard (001) orientation were synthesized by pulsed laser evaporation [16].

The original target (the sintered ceramic tablet of  $\text{Nd}_{2-x}\text{Ce}_x\text{CuO}_{4+\delta}$  of the given composition) was evaporated by a focused laser beam and the evaporated target material was deposited on a heated single-crystal substrate. The substrate material was  $\text{SrTiO}_3$  with (100) orientation and dimensions of  $5 \times 10 \times 1.5$  mm. The substrate temperature was  $800^\circ\text{C}$ , the pressure during the deposition was 1.067 mbar, the residual gas was nitrous oxide ( $\text{N}_2\text{O}$ ). Then the films were subjected to heat treatment (annealing) under various conditions to obtain samples with various oxygen content. As a result, three types of samples with  $x=0.15$  were obtained: as-grown samples, optimally reduced samples (optimally annealed in a vacuum at  $T = 780^\circ\text{C}$  for  $t = 60$  min;  $p = 1.33 \cdot 10^{-2}$  mbar) and non optimally reduced samples (annealed in a vacuum  $T = 780^\circ\text{C}$  for  $t = 40$  min;  $p = 1.33 \cdot 10^{-2}$  mbar). Temperature dependence of resistivity were measured at the magnetic field up to 90 kOe using the Quantum Design PPMS in the temperature range  $T = (1.8 \div 300)$  K and the Oxford Instruments superconducting magnet up to 120 kOe in the temperature range  $T = (0.4 \div 4.2)$  K.

### 3. EXPERIMENTAL RESULTS AND DISCUSSION

The in-plane longitudinal resistivity  $\rho_{xx}$  is measured as a function of temperature  $T$  for different applied magnetic fields  $H$  or as a function of  $H$  at fixed temperatures in single crystal films of electron-doped superconductor  $\text{Nd}_{2-x}\text{Ce}_x\text{CuO}_{4+\delta}$  in magnetic field perpendicular to the  $ab$ -plane up to 90 kOe at  $T=(0.4 \div 300)\text{K}$ . Fig.1a shows the  $\rho(T)$  dependences for the optimally reduced  $\text{Nd}_{1.85}\text{Ce}_{0.15}\text{CuO}_4$  film. It is seen that an increase of the external magnetic field results in a shift of the resistive transition to lower temperatures without appreciable broadening. Thus the values of the upper critical field  $H_{c2}$  can be deduced from  $\rho(T)$  curves for fixed magnetic fields. For the definition of  $H_{c2}$  we use a value that is the intersection of tangents to the resistive transition region and to the normal-state resistivity region (see Fig.1b).

In Fig.2 we have plotted  $H_{c2}(T)$  dependences derived from measured  $\rho(T)$  and  $\rho(B)$  transitions for all our  $\text{Nd}_{1.85}\text{Ce}_{0.15}\text{CuO}_{4+\delta}$  samples. In both optimally and nonoptimally reduced films we observe a positive curvature of  $H_{c2}(T)$  for temperatures from  $T_c$  down to about  $T_c/2$  and then obvious tendency to saturation at low temperatures.

On the insert of Fig.2  $H_{c2}(T)$  dependences for optimally and nonoptimally reduced samples of Golnik and Naito [15] are presented for comparison. It is

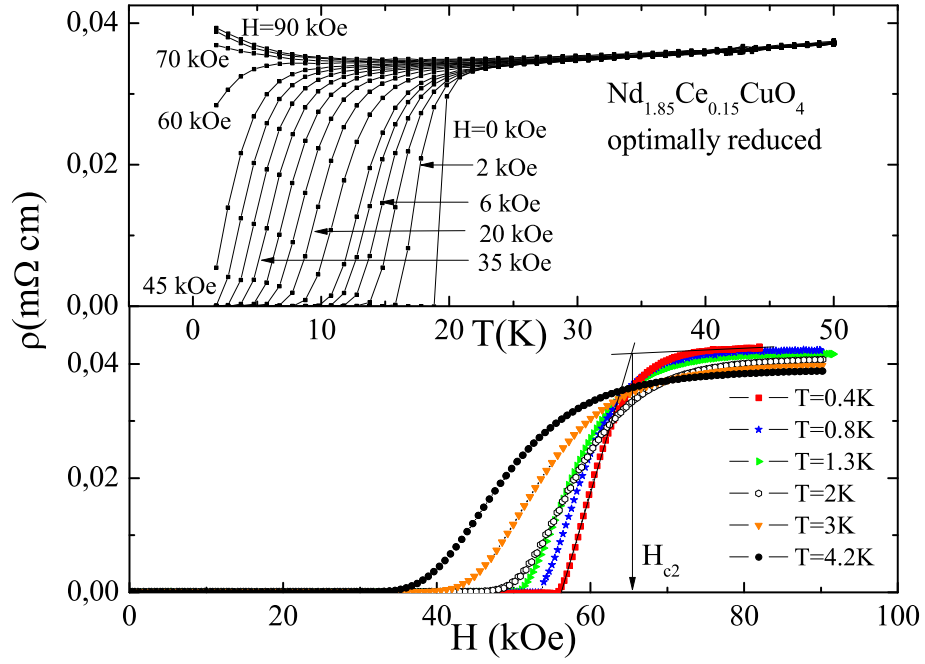


Figure 1: The resistive transitions of the  $\text{Nd}_{1.85}\text{Ce}_{0.15}\text{CuO}_4/\text{SrTiO}_3$  film with optimal annealing: (a) as function of temperature at various magnetic fields; (b) as a function of magnetic field at various temperatures.

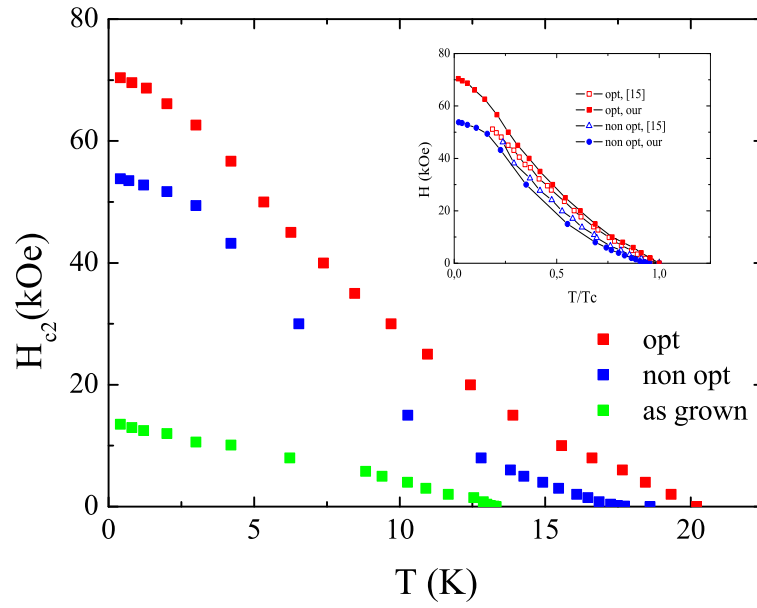


Figure 2: Temperature dependences of the upper critical field  $H_{c2}$  defined as a value of the crossing of two tangents: first - to the resistive transition region; second - to the normal resistivity region. Inset:  $H_{c2}(T)$  dependences for optimally and nonoptimally reduced samples of Golnik and Naito [15] - open labels; our experimental data of  $H_{c2}(T)$  at  $T < 4.2\text{K}$  - solid labels.

seen that their and our dependences have similar behavior at  $T > 4.2\text{K}$  and that our data rather well complement the data of [15] at  $T < 4.2\text{ K}$ . Measurements of the resistive critical field of  $\text{Nd}_{1.84}\text{Ce}_{0.16}\text{CuO}_{4+\delta}$  single crystals have been reported for temperatures below  $4.2\text{ K}$  with similar results (see [12,13]).

As revealed by ARPES [18,19] the two types of carriers with opposite charges in the normal state of electron-doped cuprate comes from two parts of FS that is associated with a reconstruction of conduction band due to SDW ordering which splits the band into upper and lower branches [25, 26]. The inset of Fig. 3a shows the FSs for a typical optimally-doped sample [22]. The SDW correlation splits the continuum FS into two pieces of sheet: electron-like(1) and hole-like (2) pockets.

In the SC state the reconstruction of Fermi surface leads naturally to a two-gap model. The situation with piecewise FS (with two types of FS parts) in superconducting state of electron doped cuprates is properly considered, for example, by Liu and Wu [22]. The model suggests two SC gaps with different amplitude:  $\Delta_1$  for electron-like band and  $\Delta_2$  for hole-like one. The two-gap model gives a unified explanation for the experimental data on ARPES [19] and Raman scattering [27] in the electron-doped cuprates with  $x < 0.17$ .

On these grounds we explore theoretical considerations about temperature dependence of the upper critical field in two-gap superconductor [4] for an interpretation of our experimental data.

We regard  $\text{Nd}_{2-x}\text{Ce}_x\text{CuO}_{4+\delta}$  single crystal with  $x= 0.15$  as a superconductor with two sheets (pockets) 1 and 2 of the Fermi surface on which the superconducting gaps take the values  $\Delta_1$  and  $\Delta_2$ , respectively (indices 1 and 2 correspond to electron and hole pockets) and the intraband diffusivities electron  $D_1$  and hole  $D_2$ .

The equation for  $H_{c2}$  for two-band/ two-gap superconductor in the dirty limit are derived in [4] with the account of both intraband and interband scattering by nonmagnetic impurities and paramagnetic effects. For a simpler case of negligible interband scattering and paramagnetic effects the equation for  $H_{c2}$  has been presented as [4b]:

$$\ln(t) = -[U(h) + U(\eta h) + \lambda_0/w]/2 + \\ + [(U(h) - U(\eta h) - \lambda_-/w)^2/4 + \lambda_{12}\lambda_{21}/w^2]^{1/2}. \quad (1)$$

Here  $t = T/T_c$ ,  $h=H_{c2}D_1/2\Phi_0T$ ,  $\Phi_0 = \pi\hbar/e$  - is a flux quantum,  $\eta =$

$D_2/D_1$ ,

$$U(x) = \psi(1/2 + x) - \psi(1/2), \quad (2)$$

where  $\psi(x)$  is a digamma function and  $\lambda_{\pm} = \lambda_{11} \pm \lambda_{22}$ ,  $w = \lambda_{11}\lambda_{22} - \lambda_{12}\lambda_{21}$ ,  $\lambda_0 = (\lambda_{-}^2 + 4\lambda_{12}\lambda_{21})^{1/2}$ .

Eq.(1) contains the matrix of the BCS coupling constants: the diagonal terms  $\lambda_{11}$  and  $\lambda_{22}$  describe intraband pairing (band 1 have the highest coupling constant  $\lambda_{11}$ ) and  $\lambda_{12}$  and  $\lambda_{21}$  describe interband coupling.

For equal diffusivities,  $\eta = 1$ , Eq. (1) simplifies to the one-gap de-Gennes-Maki equation of Werthamer - Helfand - Hohenberg (WHH) theory (see [28] and references therein):

$$\ln(t) + U(h) = 0. \quad (3)$$

As was to be expected for  $\lambda_{12}=0$  equation (1) breaks up on two independent WHH ones. For the first type of carriers with  $D=D_1$  we have:

$$\ln(t^{(1)}) + U(h) = 0, \quad (4)$$

where  $t^{(1)} = T/T_c^{(1)}$ ,  $T_c^{(1)} \sim \exp(-1/\lambda_{11})$ . For the second type with  $D=D_2$  we obtain from (1):

$$\begin{aligned} \ln(t^{(1)}) + U(\eta h) &= \lambda_0/w, \\ &\text{or} \\ \ln(t^{(2)}) + U(\eta h) &= 0, \end{aligned} \quad (5)$$

where  $t^{(2)} = T/T_c^{(2)}$ ,  $T_c^{(2)} \sim \exp(-1/\lambda_{22})$  and expressions  $\lambda_0/w = (\lambda_{11} - \lambda_{22})/(\lambda_{11}\lambda_{22})$  and  $T_c^{(2)}/T_c^{(1)} = \exp(-(\lambda_{11} - \lambda_{22})/(\lambda_{11}\lambda_{22}))$ , reliable at  $\lambda_{12} = 0$ , are used.

On Figs 3, 4 we show the fit of the two-band theoretical equation (1) to  $H_{c2}(T)$  curves with fitting parameters listed in Table I for optimally (Fig. 3a) and non optimally (Fig. 4a) reduced  $\text{Nd}_{1.85}\text{Ce}_{0.15}\text{CuO}_{4+\delta}$  samples. We find that for both samples the curves of  $H_{c2}(T)$  can be rather well described by the two-band model for the diffusivity ratio  $\eta = D_2/D_1 < 1$  and for nearly negligible interband BCS coupling constants:  $\lambda_{12} \ll \lambda_{11}, \lambda_{22}$ . It follows from the previous transport measurements on two investigated samples [24] that carriers with the higher diffusivity  $D_1$  are electrons and ones with the lower diffusivity  $D_2$  are holes.



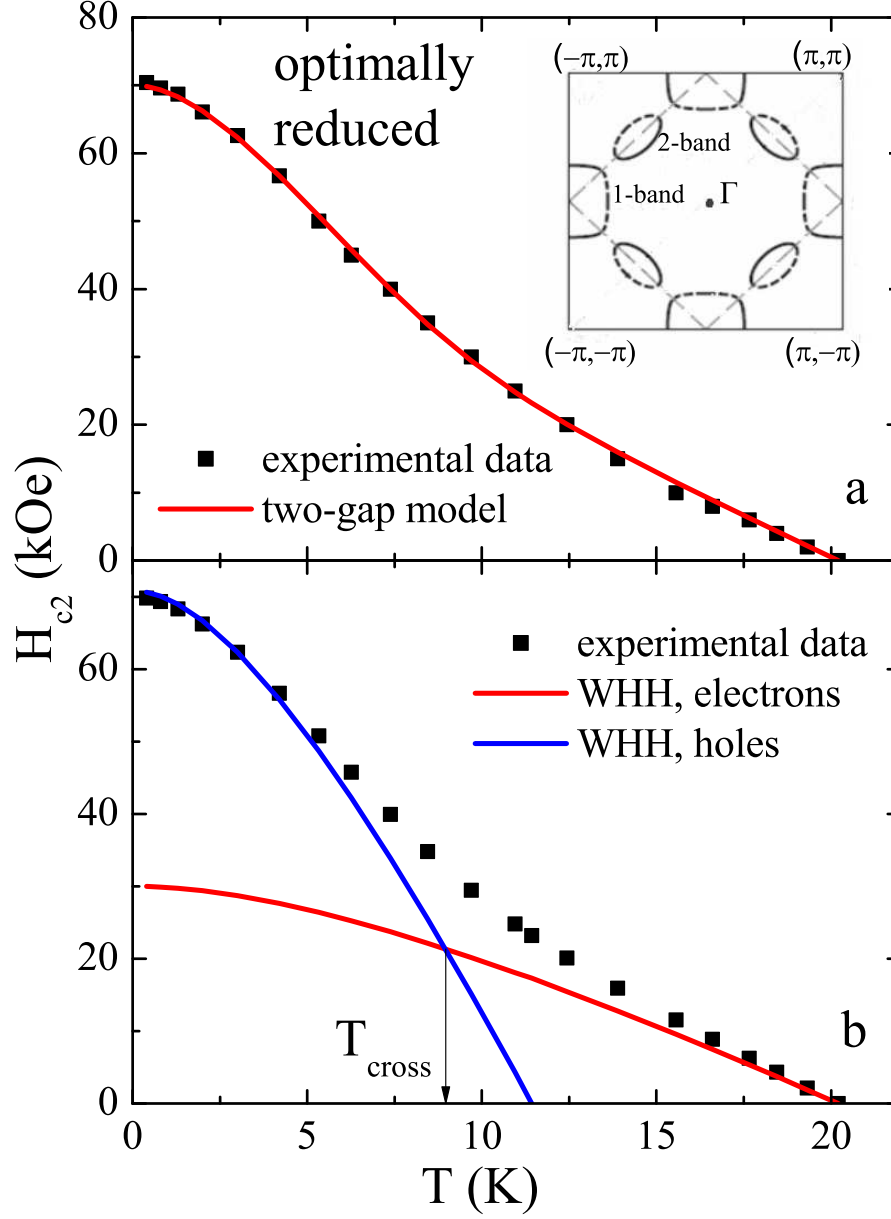


Figure 3: Upper critical field versus temperature for optimally reduced  $\text{Nd}_{1.85}\text{Ce}_{0.15}\text{CuO}_4$  sample. The filled symbols correspond to the experimental data. (a) Solid line corresponds to  $H_{c2}(T)$  calculated from the two-gap Eq.(1) for the fitting parameters listed in Table 1. (b) Red and blue curves are calculated according to the one-gap Eqs (4) and (5), respectively. The fitting parameters are listed in Table 2.

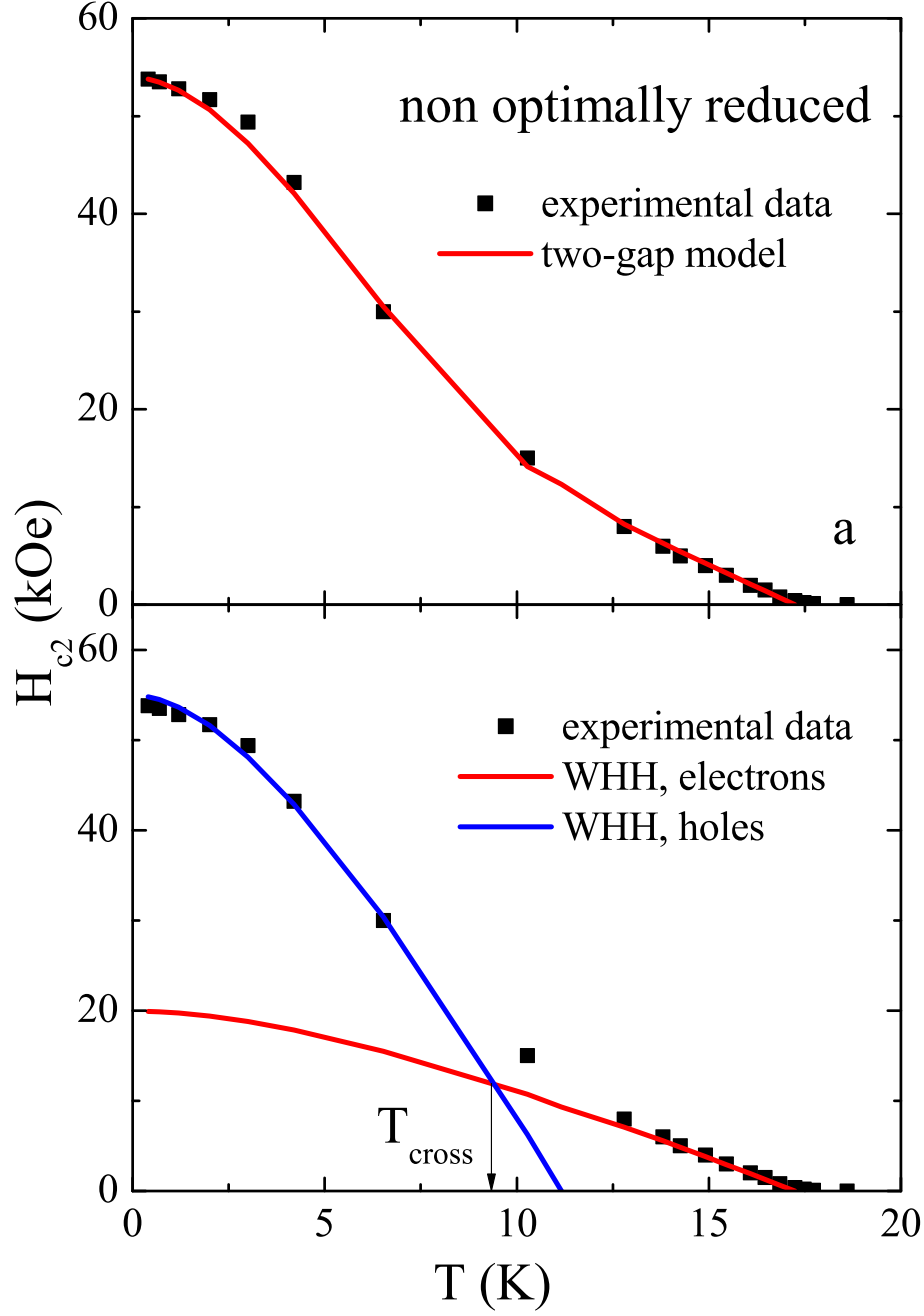


Figure 4: Upper critical field versus temperature for non optimally reduced  $\text{Nd}_{1.85}\text{Ce}_{0.15}\text{CuO}_{4+\delta}$  sample. The filled symbols correspond to the experimental data. (a) Solid line corresponds to  $H_{c2}(T)$  calculated from the two-gap Eq.(1) for the fitting parameters listed in Table 1. (b) Red and blue curves are calculated according to the one-gap Eqs (4) and (5), respectively. The fitting parameters are listed in Table 2.

Encouraging by the strong inequality between interband and intraband coupling constants we try to describe  $H_{c2}(T)$  dependences on the ground of independent equations (4) and (5) for  $\lambda_{12} = 0$ . The fitting for optimally (Fig. 3b) and non optimally (Fig. 4b) reduced samples shows that the observed dependences may be considered as a superposition of WHH-like curves for two types of carriers (electrons and holes) with different critical fields  $H_{c2}^{(1)}$  or  $H_{c2}^{(2)}$  and with different critical temperatures  $T_c^{(1)}$  or  $T_c^{(2)}$ . The fitting parameters are presented in Table 2. As it is seen from Figs. 3b and 4b it is necessary to take into account the finite value of  $\lambda_{12}$  only near a crossover of the two WHH curves at  $T = T_{cross}$ .

In accordance with analysis of Gurevich [4] in a case of different diffusivities the limiting value of  $H_{c2}(0)$  is determined by the minimum diffusivity (i.e. by holes):

$$H_{c2}(0) = \Phi_0 T_c^{(2)} / 2\gamma D_2, \quad (6)$$

where  $\gamma \cong 1.78$ . On the other hand the expressions for  $H_{c2}(T)$  near  $T_c$  is determined by the band with the highest coupling constant  $\lambda_{11}$  (i.e. by electrons):

$$H_{c2}(T) = 4\Phi_0(T_c - T)/\pi^2 D_1. \quad (7)$$

The experimentally observed ("real") values of  $H_{c2}$  and  $T_c$  should be the highest ones: for critical fields these are  $H_{c2}^{(2)}$  at  $T < T_{cross}$  and  $H_{c2}^{(1)}$  at  $T > T_{cross}$ , for critical temperature  $T_c = T_c^{(1)}$  (see Figs 3b, 4b). The lower ("virtual" in terms of the article [4b]) values of  $H_{c2}$  come to the light, for example, in the magnetic field dependences of Hall coefficient,  $R_H(B)$ , in a mixed state of superconductor (see [24]).

On Fig.5 we present the data for  $H_{c2}(T)$  dependences in as grown  $\text{Nd}_{1.85}\text{Ce}_{0.15}\text{CuO}_{4+\delta}$  sample. In contrast to the other two samples we observe here a convex form of  $H_{c2}(T)$  curve at all temperature interval. The data are remarkably well described by the WHH-like equation in accordance with a result of transport measurements [24] that electrons and holes give nearly equal contributions to the conductivity in this sample, i.e.  $D_1 \cong D_2$ . It is known [4] that for equal diffusivities of the two bands, i.e.,  $\eta = D_2/D_1 = 1$ , the parametric equation (1) reduces to the one-gap formula in the WHH theory.

From an analysis of  $R_H(B)$  dependences in a mixed state [24] we have obtained that in as grown sample the critical field for electrons is higher than that for holes:  $H_{c2}^{(1)} > H_{c2}^{(2)}$ , and both real ( $H_{c2}^{(1)}$ ) and virtual ( $H_{c2}^{(2)}$ ) fields have

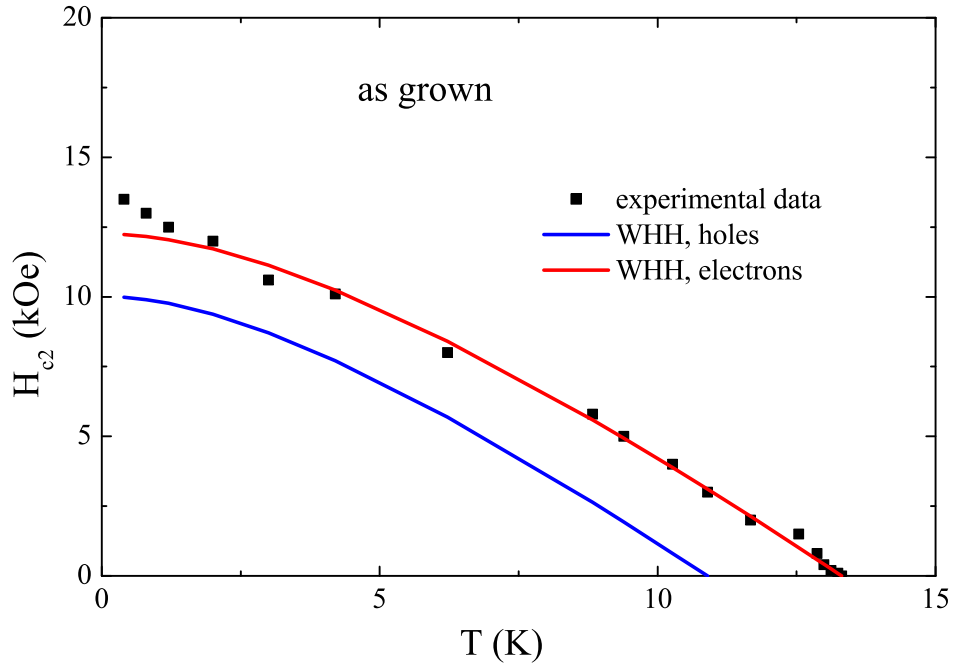


Figure 5: Upper critical field versus temperature for as grown  $\text{Nd}_{1.85}\text{Ce}_{0.15}\text{CuO}_{4+\delta}$  sample. The filled symbols correspond to the experimental data. Red and blue curves are calculated according to the WHH formulas (4) and (5), respectively. The fitting parameters are listed in Table 2.

been determined (see Table 2). As for equal diffusivities one has  $T_c^{(2)}/T_c^{(1)} = H_{c2}^{(2)}/H_{c2}^{(1)}$ , we can construct not only real WHH curve for electrons but also virtual one for holes (see Fig.5).

It should be noted that the existence of two different spatial and magnetic field scales, consistent with the experimental data on Abrikosov vortex structure in  $\text{MgB}_2$ , has been demonstrated by Koshelev and Golubov [29].

They provided a quantitative model for the vortex structure in a two-band superconductor with weak interband impurity scattering and strong intraband scattering rates. It was shown that in a case of weak interband scattering the two typical sizes of the isolated vortex in different bands appear and, as a consequence, two magnetic field scales exist which can be accessible experimentally.

#### 4. CONCLUSIONS

In conclusion, we report the data for the upper critical field as a function of temperature for  $\text{Nd}_{1.85}\text{Ce}_{0.15}\text{CuO}_{4+\delta}$  single crystal films with different degree of disorder ( $\delta$ ) determined by the resistivity measurements. Two types of  $H_{c2}(T)$  dependences are observed: the abnormal ones with a positive curvature of  $H_{c2}(T)$  for temperatures from  $T_c$  down to about  $T_c/2$  in both optimally and non optimally reduced films and conventional WHH curve in as grown film. We find that the  $H_{c2}(T)$  dependences can be consistently explained by the two-band/two-gap model of a dirty superconductor for the diffusivity ratio  $\eta = D_2/D_1 < 1$  in the first two films and for equal diffusivities,  $\eta = D_2/D_1 = 1$ , in the third one.

Thus, we have demonstrated that the two-band/two-gap model captures the essence of the behavior of  $H_{c2}(T)$  for investigated systems. This result is in accordance with experimental evidences and theoretical considerations for a coexistence of electrons and holes in a normal state of optimally doped  $\text{Nd}_{2-x}\text{Ce}_x\text{CuO}_{4+\delta}$  system.

This work was done within RAS Program (project N 12-P-2-1018) with partial support of RFBR (grant N 12-02-00202).

#### REFERENCES

#### References

- [1] H. Suhl, B.T. Matthias, and L.R. Walker, Phys. Rev. Lett.**3**, 552 (1959).

- [2] A. Y. Liu, I. I. Mazin, and J. Kortus, Phys. Rev. Lett. **87**, 87005 (2001).
- [3] S. V. Shulga et. al., cond-mat/0103154.
- [4] (a) A. Gurevich, Phys. Rev. B **67** 184515 (2003); (b) A. Gurevich, Physica C **456**, 160 (2007).
- [5] Y. Kamihara, T. Watanabe, M. Hirano, and H. Hosono: J. Am. Chem.Soc. **130** 3296 (2008).
- [6] I. I. Mazin, D. J. Singh, M. D. Johannes, and M. H. Du: Phys. Rev.Lett. **101** 057003 (2008).
- [7] J. Jaroszynski, F. Hunte, L. Balicas, Youn-jung Jo, I. Raicevich, A. Gurevich, and D. C. Larbalestier, F. F. Balakirev, L. Fang, P. Cheng, Y. Jia, and H. H. Wen, Phys. Rev. B **78**, 174523 (2008).
- [8] F. Hunte, J. Jaroszynski, A. Gurevich, D. C. Larbalestier, R. Jin, A. S. Sefat, M. A. McGuire, B. C. Sales, D. K. Christen, D. Mandrus, Nature (London) **453**, 903 (2008).
- [9] S. A. Baily, Y. Kohama, H. Hiramatsu, B. Maierov, F. F. Balakirev, M. Hirano, and H. Hosono, Phys. Rev. Lett. **102**, 117004 (2009).
- [10] M. Kano, Y. Kohama, D. Graf, F. Balakirev, A. S. Sefat, M. A. McGuire, B. C. Sales, D. Mandrus, and S. W. Tozer, J. Phys. Soc. Jpn. **78**, 084719 (2009).
- [11] Rongwei Hu, Eun Deok Mun, M. M. Altarawneh, C. H. Mielke, V. S. Zapf, S. L. Bud'ko, and P. C. Canfield, Phys. Rev. B **85**, 064511 (2012).
- [12] Y. Hidaka and M. Suzuki, Nature (London) **338**, 635 (1989).
- [13] Y. Dalichaouch, B. W. Lee, C. L. Seaman, J. T. Markert, and M. B. Maple, Phys. Rev. Lett. **64**, 599 (1990).
- [14] V.F.Gantmacher, G.A. Emel'chenko, I.G. Naumenko, G.E. Tsydynzhapov, JETP Letters **72**, 21 (2000).
- [15] F. Gollnik, M. Naito, Phys. Rev. B **58**, 11734 (1998).
- [16] T. B. Charikova, N. G. Shelushinina, G. I. Kharus, and A.A.Ivanov, JETP Letters **88**, 123 (2008).

- [17] N.Luo, arXiv:cond-mat/0003074v2.
- [18] N. P. Armitage, F. Ronning, D. H. Lu, C. Kim, A. Damascelli, K. M. Shen, D. L. Feng, H. Eisaki, and Z.-X. Shen, P. K. Mang, N. Kaneko, and M. Greven, Y. Onose, Y. Taguchi, and Y. Tokura, Phys.Rev.Lett. **88**, 257001 (2002); N.P.Armitage, P. Fournier, and R. L. Greene, Rev.Mod.Phys. **82**, 2421 (2010).
- [19] H. Matsui, K. Terashima, T. Sato, T. Takahashi, S.-C. Wang, H.-B. Yang, H. Ding, T. Uefuji, and K. Yamada, Phys.Rev.Lett. **94**, 047005 (2005); H. Matsui, K. Terashima, T. Sato, T. Takahashi, M. Fujita, and K. Yamada, Phys.Rev.Lett. **95**, 017003 (2005).
- [20] M. Ikeda, T. Yoshida, A. Fujimori, M. Kubota, K. Ono, K. Unozawa, T. Sasagawa, H. Takagi, J.Supercond.Nov.Magn. **20**, 563 (2007); M. Ikeda, T. Yoshida, A. Fujimori, M. Kubota, K. Ono, Hena Das, T.Saha-Dasgupta, K. Unozawa, Y. Kaga, T. Sasagawa, and H. Takagi, Phys.Rev.B **80**, 014510 (2009).
- [21] J. Lin and A. J. Millis, Phys.Rev.B **72**, 214506 (2005).
- [22] C. S. Liu and W. C. Wu, Phys.Rev.B **76**, 014513 (2007), Figs.1c,d.
- [23] E. Z.Kuchinskii, M.V. Sadovskii, JETP Letters **88**, 224 (2008).
- [24] T.B. Charikova, N.G. Shelushinina, G.I. Harus, D.S. Petukhov, A.V. Korolev, V.N. Neverov, A.A. Ivanov, Physica C **483**, 113 (2012).
- [25] C. Kusko, R. S. Markiewicz, M. Lindroos, and A. Bansil, Phys. Rev. B **66**, 140513(R) (2002).
- [26] Q. Yuan, Y. Chen, T. K. Lee, and C. S. Ting, Phys. Rev. B **69**, 214523 (2004).
- [27] G. Blumberg, A. Koitzsch, A. Gozar, B. S. Dennis, C. A. Kendziora, P. Fournier, and R. L. Greene, Phys. Rev. Lett. **88**, 107002 (2002).
- [28] N.R. Werthamer, E. Helfand, P.C. Hohenberg, Phys. Rev. **147**, 295 (1966).

- [29] A. E. Koshelev A. A. Golubov , Phys. Rev. Lett. **90**, 177002 (2003). An equation (11) of [29] is similar to Eq. (34) reported in Ref. 4(a) or Eq. (25) of Ref. 4(b) (see Eq. (1) in our work).

new page

Table 1: Parameters of the fits to the two-gap formula (1) for  $\text{Nd}_{1.85}\text{Ce}_{0.15}\text{CuO}_{4+\delta}/\text{SrTiO}_3$  epitaxial films.

Samples	$T_c$ , K	$H_{c2}(0)$ , kOe	$\begin{pmatrix} \lambda_{11}\lambda_{12} \\ \lambda_{21}\lambda_{22} \end{pmatrix}$	$D_1$	$D_2$	$\eta$
Optimally reduced	20.2	70.4	$\begin{pmatrix} 0.43 & 0.044 \\ 0.044 & 0.35 \end{pmatrix}$	1.89	0.45	0.24
Non optimally reduced	17.3	53.8	$\begin{pmatrix} 0.54 & 0.038 \\ 0.038 & 0.44 \end{pmatrix}$	2.43	0.57	0.235



Table 2: Parameters of the fits to the WHH-like formulas (4) and (5) for  $\text{Nd}_{1.85}\text{Ce}_{0.15}\text{CuO}_{4+\delta}/\text{SrTiO}_3$  epitaxial films.

Samples	$T_c^{(1)}$ , K	$H_{c2}^{(1)}(0)$ , kOe	$T_c^{(2)}$ K	$H_{c2}^{(2)}(0)$ kOe	$D_1$	$D_2$	$\eta$
Optimally reduced	20.2	30.0	11.4	70.4	1.89	0.45	0.24
Non optimally reduced	17.3	20.0	11.2	53.8	2.43	0.57	0.235
As grown	13.3	12.2	10.9	10.0	3.0	3.0	1